Acta Crystallographica Section D
**Biological Crystallography**
ISSN 1399-0047

# Structural analysis of the endogenous glycoallergen Hev b 2 (endo-$\beta$-1,3-glucanase) from *Hevea brasiliensis* and its recognition by human basophils

**Adela Rodríguez-Romero,[a]* Alejandra Hernández-Santoyo,[a] Deyanira Fuentes-Silva,[a] Laura A. Palomares,[b] Samira Muñoz-Cruz,[c] Lilian Yépez-Mulia[c] and Socorro Orozco-Martínez[d]**

[a]Instituto de Química, Universidad Nacional Autónoma de México, Circuito Exterior, CU, 04310 Coyoacán, DF, Mexico, [b]Instituto de Biotecnología, Universidad Nacional Autónoma de México, Apartado Postal 510-3, 62250 Cuernavaca, MOR, Mexico, [c]UMAE–Hospital de Pediatría, Centro Médico Nacional Siglo XXI, IMSS, Avenida Cuauhtémoc 330, Colonia Doctores, Mexico, DF, Mexico, and [d]Instituto Nacional de Pediatría, Insurgentes Sur 3700C, 04530 Cuicuilco, DF, Mexico

Correspondence e-mail: adela@unam.mx

Received 11 July 2013
Accepted 9 October 2013

**PDB references:** Hev b 2, 4hpg; 4iis

Endogenous glycosylated Hev b 2 (endo-$\beta$-1,3-glucanase) from *Hevea brasiliensis* is an important latex allergen that is recognized by IgE antibodies from patients who suffer from latex allergy. The carbohydrate moieties of Hev b 2 constitute a potentially important IgE-binding epitope that could be responsible for its cross-reactivity. Here, the structure of the endogenous isoform II of Hev b 2 that exhibits three post-translational modifications, including an N-terminal pyro-glutamate and two glycosylation sites at Asn27 and at Asn314, is reported from two crystal polymorphs. These modifications form a patch on the surface of the molecule that is proposed to be one of the binding sites for IgE. A structure is also proposed for the most important *N*-glycan present in this protein as determined by digestion with specific enzymes. To analyze the role of the carbohydrate moieties in IgE antibody binding and in human basophil activation, the glycoallergen was enzymatically deglycosylated and evaluated. Time-lapse automated video microscopy of basophils stimulated with glycosylated Hev b 2 revealed basophil activation and degranulation. Immunological studies suggested that carbohydrates on Hev b 2 represent an allergenic IgE epitope. In addition, a dimer was found in each asymmetric unit that may reflect a regulatory mechanism of this plant defence protein.

## 1. Introduction

Type I IgE-mediated natural rubber latex (NRL) hypersensitivity has been studied in detail in the US and the European community over the past two decades (Garabrant *et al.*, 2001; Bousquet *et al.*, 2006; Peixinho *et al.*, 2012) and continues to be an important occupational health problem, despite significant progress in the management of the disease (Blumchen *et al.*, 2010). The prevalence of IgE-mediated NRL allergy among healthcare workers has been estimated to be 3–17%, but is higher in individuals with spina bifida and in those who have had multiple surgeries (Bousquet *et al.*, 2006; Cremer *et al.*, 2007). In less industrialized countries, NRL allergic sensitization remains a serious clinical concern (Buss & Fröde, 2007; Kumar, 2012), although its prevalence is often not documented. Among the 14 NRL allergens listed by The World Health Organization and International Union of Immunological Societies Allergen Nomenclature Committee (http://www.allergen.org), Hev b 2 (endo-$\beta$-1,3-glucanase) has been reported to be an important allergen that is recognized by IgE antibodies in patients suffering from type I latex hypersensitivity (Bernstein *et al.*, 2003; Yagami *et al.*, 2002). This allergen has also been implicated in serological cross-reactivity between pollens, vegetable foods and insect venoms (Palomares *et al.*, 2005; Barre *et al.*, 2009; Mahler *et al.*, 2006). In higher plants, $\beta$-1,3-glucanases play a critical role in protection

against phytopathogenic fungi, either alone or in association with chitinases, and they are also important for diverse physiological processes in uninfected plants, including pollen development, germination of seeds and cell division (Balasubramanian *et al.*, 2012).

In lutoid extracts from *Hevea brasiliensis* latex, $\beta$-1,3-glucanase exists as two basic isozymes that are differentially N-glycosylated (Churngchow *et al.*, 1995). We have previously reported the carbohydrate contents and saccharide compositions of these two isoforms of Hev b 2 (Fuentes-Silva *et al.*, 2007). Isoforms I and II contain 20 and 6%(*w*/*w*) carbohydrate content, respectively. Isoform I includes *N*-acetylglucosamine (GlcNAc), *N*-acetylgalactosamine (GalNAc), fucose (Fuc) and galactose (Gal) residues as the major saccharides. Isoform II contains *N*-acetylglucosamine, fucose, mannose (Man) and xylose (Xyl). Recent studies have demonstrated that allergens with complex *N*-glycans containing L-Fuc($\alpha$1$\rightarrow$3), D-Xyl($\beta$1$\rightarrow$2) (van Ree *et al.*, 2000; Fötisch & Vieths, 2001) and more recently Gal($\alpha$1$\rightarrow$3) are recognized by IgE antibodies (Plum *et al.*, 2011) and are prone to extensive cross-reactivity against carbohydrate determinants (CCDs) from unrelated sources (Foetisch *et al.*, 2003; Bonds *et al.*, 2008; Tretter *et al.*, 1993). Nevertheless, the role of *N*-glycan-specific IgEs in allergic reactions remains controversial. Moreover, the release of histamine from basophils and mast cells that plays a central role in type I hypersensitivity (Gauchat *et al.*, 1993; Galli *et al.*, 2005; Sokol *et al.*, 2008) and in parasitic infections (Min *et al.*, 2004) is also a complex biochemical process, but little information concerning the histamine-releasing activity of such CCDs is available. A few histamine-release studies have indicated that the carbohydrate moieties of glycoallergens could trigger basophil and mast-cell degranulation, suggesting that these sugars might indeed be biologically active in allergic responses (Iacovacci *et al.*, 2002; Westphal *et al.*, 2003; Batanero *et al.*, 1999). Recently, the crystal structure of the IgG Fab of the monoclonal antibody 4C3 against Bla g 2 in complex with the recombinant glycosylated allergen clearly demonstrated the contribution of the glycan moieties to the interaction (Glesner *et al.*, 2011). The authors observed that a trimannosyl core at residue Asn268 primarily interacted with CDRs H1 and H2 of the antibody, essentially through contacts that were mediated by water molecules and ions. Moreover, it has been shown that diverse glycosylated allergens are internalized by the mannose receptor that is expressed in dendritic cells (Royer *et al.*, 2010), thus playing a crucial role in allergen-induced Th2 cell polarization. Nevertheless, the three-dimensional structures of endogenous glycoallergens from plants have thus far not been reported, which may relate to the requirement for the purification of glycosylated isoforms that are often isolated in minuscule amounts and/or are heterogeneous in nature and whose covalently bound oligosaccharides can negatively influence the solubility and crystallizability of the proteins. Here, we report the molecular structure of the endogenous glycosylated isoform II of Hev b 2, a $\beta$-1,3-glucanase from *H. brasiliensis*, from two polymorphic crystals. Electron-density maps revealed three post-translational modifications located as a patch on the surface of the molecule. Time-lapse automated video microscopy of basophils stimulated with glycosylated and deglycoslylated Hev b 2 indicated greater basophil activation with the glycosylated Hev b 2. Our results based on immunological and structural analyses imply that the carbohydrate moieties on the surface of Hev b 2 constitute an important epitope that is recognized by IgE antibodies in the sera of allergic patients.

## 2. Materials and methods

### 2.1. Protein purification, crystallization and data collection

The endogenous glycosylated isoform II of Hev b 2 was purified and crystallized using previously described protocols (Fuentes-Silva *et al.*, 2007). Briefly, the enzyme was isolated and purified from the lutoids of *H. brasiliensis* latex (clone GV-42) using gel filtration on a HiLoad 16/20 Superdex 200 column and affinity chromatography with concanavalin A (Con A) Sepharose 4B (Pharmacia-LKB Biotechnology, Sweden). Both the bound and the non-bound fractions from the Con A chromatography showed $\beta$-1,3-glucanase activity. Each isoform was purified to homogeneity by cation-exchange chromatography with a Mono S 5/50 GL column (Pharmacia): the non-bound fraction was named isoform I, while the bound fraction was named isoform II (Churngchow *et al.*, 1995). Samples were dialyzed, concentrated to 6 mg ml$^{-1}$ and used for crystallization. Diffraction-quality crystals of Hev b 2 isoform II were obtained using two conditions from Crystal Screen (Hampton Research, Laguna Niguel, USA) and the hanging-drop vapour-diffusion method. In the first condition, 0.2 *M* trisodium citrate, 0.1 *M* sodium cacodylate pH 6.5, 30%(*v*/*v*) 2-propanol was used to obtain tetragonal crystals. In the second condition, good-quality monoclinic crystals grew using 0.2 *M* ammonium acetate, 0.1 *M* trisodium citrate pH 5.6, 30%(*w*/*v*) polyethylene glycol 4000 (Fuentes-Silva *et al.*, 2007). The monoclinic space group $P2_1$ was confirmed by *POINTLESS* (Evans, 2006).

X-ray diffraction data for the tetragonal polymorph were collected on beamline X6A at the National Synchrotron Light Source (NSLS), Upton, New York, USA under cryogenic conditions at 100 K using 35%(*w*/*v*) trehalose as cryoprotectant. A Quantum 210 CCD detector (Area Detector System Corporation, Poway, California, USA) was used with an oscillation range $\Delta\varphi$ of 1.0°. For the monoclinic crystal, data were collected at 100 K on the Dupont Northwestern Dow and Life Science Collaborative Access Team station at the Advanced Photon Source (APS), Argonne National Laboratory, Illinois, USA. Data sets were integrated using *XDS* (Kabsch, 2010) and were scaled with *SCALA* v.3.3.20 (Evans, 2006).

The tetragonal crystal data were initially processed and scaled in space group *P*422, with unit-cell parameters $a$ = 150.24, $b$ = 150.24, $c$ = 77.48 Å; however, the refinement statistics remained poor ($R_{\rm cryst}$ and $R_{\rm free}$ of 0.28 and 0.43, respectively). Re-examination of the original data with *phenix.xtriage* suggested that the crystal was twinned with a merohedral twinning fraction of 0.44 (twin law $h$, $-k$, $-l$), and

the actual space group was determined to be $P4_1$ with four molecules in the asymmetric unit. *DATAMAN* (Padilla & Yeates, 2003) confirmed that the crystal was twinned (Supplementary Fig. S1[1]).

### 2.2. Structure determination and refinement

Initial phases for the monoclinic $P2_1$ crystal were determined by the molecular-replacement method with *Phaser* v.2.1 (McCoy *et al.*, 2007) using the atomic coordinates of the recombinant banana endo-$\beta$-1,3-glucanase (PDB entry 2cyg; Receveur-Bréchot *et al.*, 2006), which shares 60% sequence identity with isoform II of the *H. brasiliensis* protein. All of the refinement steps were performed with *PHENIX* (Adams *et al.*, 2010). The initial molecular-replacement solution (TFZ = 19.1 and log-likelihood gain = 17 444) was refined using rigid-body refinement; noncrystallographic symmetry (NCS) restraints were then applied. The resulting model underwent iterative cycles of refinement and manual rebuilding with *Coot* (Emsley *et al.*, 2010). At the final stages of the refinement process, the NCS restraints were removed from the protocol. Carbohydrates were located on the basis of electron density, suitable interactions and the oligosaccharide sequence obtained biochemically (details below). The correct stereochemistry and chirality of the oligosaccharides were corroborated using the *Glycam Biomolecule Builder* (http://glycam.ccrc.uga.edu). The second crystal form ($P4_1$ polymorph) diffracted to lower resolution and merohedral twinning was also detected with *phenix.xtriage* and *DATAMAN* (Padilla & Yeates, 2003). The coordinates of monomer *A* of the refined monoclinic structure were used as a model for molecular replacement. For refinement the protocol described above was used but including the twin law $h, -k, -l$ and the twin fraction (0.44) in *phenix.refine*. The final structures satisfied the *MolProbity* (Chen *et al.*, 2010) criteria at corresponding resolutions. All molecular-graphics representations were drawn using *Chimera* (Pettersen *et al.*, 2004) and *PyMOL* v.1.3 (Schrödinger).

### 2.3. Deglycosylation of Hev b 2

Endogenous Hev b 2 (isoform II) was deglycosylated, without denaturation, using the NDEGLY enzymatic deglycosylation kit (Sigma, St Louis, Missouri, USA) according to the manufacturer's specifications. The integrity of the dialyzed protein after deglycosylation was verified by means of the enzymatic activity using laminarin as a substrate and the dinitrosalicylic acid (DNS) method (Miller, 1959).

### 2.4. Analysis of the N-linked glycan structures

The N-linked oligosaccharides from denatured Hev b 2 were released by digestion with peptide-*N*-glycosidase F from *Chryseobacterium meningosepticum* or with peptide-*N*-glycosidase A from almond (Calbiochem, San Diego, California, USA). Glycans were labelled with 2-aminobenzamide using the Signal 2AB labelling kit (Glyko Inc., Novato, California, USA) according to the manufacturer's specifications. Labelled glycans were separated by HPLC with a GlycoSep N column utilizing a gradient of acetonitrile and 250 m*M* ammonium formate pH 4.4 as previously described (Guile *et al.*, 1997). Separated glycans were detected with a fluorescence detector, with excitation and emission wavelengths of 330 and 420 nm, respectively. Glucose units (GU) were assigned to the observed peaks by comparison with a glucose homopolymer standard (Glyco Inc.). The structure of the glycans was assessed considering their GU and their susceptibility to exoglycosidases such as $\beta$(1–3,4,6)-galactosidase from bovine testis, $\alpha$(1–2,3,4,6)-fucosidase from bovine kidney, $\beta$(1–2,3,4,6)-*N*-acetylhexosaminidase and $\alpha$(1–2,3,6)-mannosidase from jack bean.

### 2.5. Direct ELISA assay

ELISA experiments were carried out in order to estimate the importance of the Hev b 2 carbohydrate moieties in the IgE interaction. Each well of 96-well Nunc MaxiSorp microlitre plates was coated with 100 µl (5 µg ml$^{-1}$) glycosylated or deglycosylated Hev b 2 in PBS for 1 h at 37°C. After washing with 0.1%(*v*/*v*) Tween-20 in PBS, the plates were blocked with 0.5%(*w*/*v*) gelatin in PBS for 2 h at 37°C. In order to analyze IgE antibody binding, sera of allergic donors were diluted 1:10 and 100 µl was added to the wells; the plates were then incubated for 3 h at 37°C. Five sera from non-allergic voluntary donors were used as controls. The subsequent steps included the addition of biotinylated anti-human IgE at a 1:1000 dilution to the well after a washing step, and incubation for 1 h at 37°C. The enzyme conjugate streptavidin peroxidase (1:2000) was added and incubated for 1 h at 37°C. The peroxidase reaction was developed using fresh *ortho*-phenylenediamine substrate and was stopped after 15 min by adding 50 µl 6 *N* HCl. The plates were read at 490 nm with an Elx 808 Ultra Microplate Reader. Each absorbance value was calculated as the mean of three independent determinations. The Ethics Committee of the Instituto Nacional de Pediatría, México, DF approved the protocol used to obtain sera from allergic patients.

### 2.6. *In vitro* basophil activation

Human basophils were purified from peripheral blood from non-atopic donors as described previously (Leonard *et al.*, 1984). For sensitization, the basophils were incubated for 1 h at 37°C with serum from a latex-allergic patient at a final concentration of 10%. Sensitized basophils were seeded onto 35 mm glass-bottom micro-well dishes (MatTek Co, USA) at a density of $1 \times 10^5$ in Hank's Balanced Salt Solution (HBSS) and were further stimulated with glycosylated or deglycosylated Hev b 2 at 150 ng ml$^{-1}$. Stimulation with the major latex allergen Hev b 6.02 at 75 ng ml$^{-1}$ was also included. Non-sensitized as well as non-stimulated basophils were used as negative controls.

Morphological changes were associated with basophil activation and degranulation (Xiang *et al.*, 2001) and were visualized by Nomarski differential interference contrast

[1] Supporting information has been deposited in the IUCr electronic archive (Reference: MN5038).

**Table 1**
X-ray data-collection and refinement statistics.

Values in parentheses are for the highest resolution shell.

| | Polymorph 1 | Polymorph 2 |
|---|---|---|
| Data collection | | |
| Radiation source | 5ID-B, APS | X6A, NSLS |
| Wavelength (Å) | 0.97 | 0.977 |
| Space group | $P2_1$ | $P4_1$ |
| Unit-cell parameters (Å, °) | $a$ = 87.18, $b$ = 89.78, $c$ = 101.54, $\beta$ = 113.59 | $a$ = 150.12, $b$ = 150.12, $c$ = 77.33 |
| Reflections (total/unique) | 187212/46317 | 177816/46257 |
| Resolution limits (Å) | 25.21–2.54 | 47.47–2.67 |
| Completeness (%) | 97.1 (78.92) | 93.5 (93.36) |
| $R_{\rm merge}$† (%) | 7.1 (15.3) | 7.6 (49.6) |
| $\langle I/\sigma(I)\rangle$ | 13.49 (4.96) | 10.8 (2.1) |
| Average multiplicity | 4.0 (2.9) | 3.5 (3.4) |
| $B$ factor from Wilson plot (Å$^2$) | 35.8 | 45.5 |
| Refinement statistics | | |
| Resolution (Å) | 25.21–2.54 | 47.47–2.67 |
| No. of reflections | 46317 | 46257 |
| $R/R_{\rm free}$‡ (%) | 19.3/24.1 | 20.2/22.0 |
| No. of reflections for test set | 1878 | 2352 |
| Twin law | | $h$, $-k$, $-l$ |
| Twin fraction | | 0.44 |
| No. of non-H atoms | | |
| Protein (316 residues) | 9938 | 9887 |
| Water molecules | 193 | 56 |
| No. of ligand molecules | | |
| Polyethylene glycol | 2 | 0 |
| Cacodylate ions | 0 | 1 |
| Citrate ions | 0 | 3 |
| $Na^+$ ions | 0 | 1 |
| Sugar rings | | |
| Chain $B$ | 1 GlcNAc, 1 Fuc | 0 |
| Chain $C$ | 2 GlcNAc, 1 Fuc | 2 GlcNAc |
| R.m.s. deviations | | |
| Bond lengths (Å) | 0.011 | 0.011 |
| Bond angles (°) | 1.48 | 1.63 |
| Ramachandran plot, residues in (%) | | |
| Most favoured region | 99.4 | 99.4 |
| Disallowed region | 0.6 | 0.6 |
| Clashscore from *MolProbity* | 0.03 | 0.10 |
| Average $B$ factor (Å$^2$) | 36.00 | 56.20 |
| PDB code | 4hpg | 4iis |

† $R_{\rm merge} = \sum_{hkl}\sum_i |I_i(hkl) - \langle I(hkl)\rangle|/\sum_{hkl}\sum_i I_i(hkl)$, where $\langle I(hkl)\rangle$ and $I_i(hkl)$ are the mean and the $i$th measurement of the intensity of reflection $hkl$, respectively. ‡ Crystallographic $R = \sum_{hkl}\big||F_{\rm obs}| - |F_{\rm calc}|\big|/\sum_{hkl}|F_{\rm obs}|$, where $|F_{\rm obs}|$ and $|F_{\rm calc}|$ are the observed and calculated structure-factor amplitudes, respectively. $R_{\rm free}$ is the corresponding $R$ value for a randomly chosen 5% of the reflections that were not included in the refinement.

microscopy. Live-cell time-lapse microscopy images were obtained at different times using 40×/1.3 Oil Plan-Neofluar objectives on a confocal laser scanning microscope (Zeiss, LSM 510). Images were acquired using an Zeiss AxioCam HR with *LSM 5 Image Examiner* software.

## 3. Results and discussion

### 3.1. Overall structural features of native Hev b 2

Hev b 2 is a basic, vacuolar endo-$\beta$-1,3-glucanase (glucan endo-l,3-$\beta$-D-glucosidase; EC 3.2.1.39) that belongs to family 17 of the glycoside hydrolases (GH17) and to the PR-2 family of pathogenesis-related proteins (Leubner-Metzger & Meins, 1999). Hev b 2 has also been reported to be one of the most allergenic proteins in latex from the rubber tree *H. brasiliensis* (Yeang *et al.*, 2000). The isoform II of $\beta$-1,3-glucanase used in this study was isolated from its endogenous source (*H. brasiliensis* latex, clone GV42). Therefore, we confronted two challenges in its structural studies: its degree of glycosylation and the presence of another isoform (I) that is also glycosylated but lacks a mannose core. The results presented in this study correspond to the less glycosylated enzyme (isoform II), which consists of 316 residues and was identified among the 11 nonredundant sequences that have been deposited in GenBank with accession code ABN09655.1.

As previously reported (Fuentes-Silva *et al.*, 2007), Hev b 2 isoform II crystallized in two polymorphic crystals that diffracted X-rays to 2.54 Å ($P2_1$) and 2.67 Å ($P4_1$) resolution. Both crystal forms demonstrated high solvent contents (57.2 and 62.2%, respectively), with Matthews coefficients of 2.88 Å$^3$ Da$^{-1}$ for the monoclinic crystal and 3.26 Å$^3$ Da$^{-1}$ for the tetragonal crystal, indicating that both contained four protein molecules in the asymmetric unit (*A*, *B*, *C* and *D*), although it has been reported that the protein is monomeric in solution (Churngchow *et al.*, 1995). Both polymorphs presented the 316 amino-acid residues of the mature enzyme and several saccharides that are covalently attached to two Asn residues (27 and 314) in the protein. The determination of the structure of the $P4_1$ polymorph was hindered by a combination of slightly lower resolution and the presence of merohedral twinning, as confirmed by the cumulative intensity plot (Supplementary Fig. S1); nevertheless, all of the amino acids and two saccharides on residue 27 (monomer *C*) could be interpreted in the electron-density maps. Some side chains of solvent-exposed residues were modelled as Ala in both polymorphs. Additionally, two residues (Trp104 and Asn312) in each monomer exhibit torsion angles that lie outside the expected regions in the Ramachandran plot. Trp104 is located in the Ω-like loop that lies near the substrate-binding groove and Asn312 is located near the second glycosylation site (Asn314). Electron-density maps for these two residues are shown in Supplementary Fig. S2. A summary of the refinement and final model statistics for the two Hev b 2 polymorphs are provided in Table 1 and the atomic coordinates have been deposited in the Protein Data Bank as entries 4hpg and 4iis.

As shown in Figs. 1(*a*) and 1(*b*), ribbon representations of both the monoclinic and the tetragonal lattices exhibit four protein molecules in the asymmetric unit, but the assemblies are different. The monoclinic asymmetric unit of Hev b 2 is arranged in a tetrahedral form, whereas the tetragonal asymmetric unit forms a flat square. The topology of each individual monomer is that shown in Fig. 1(*c*), which depicts the canonical $(\alpha/\beta)_8$ TIM-barrel motif that is found in other plant $\beta$-1,3-glucanases such as those from barley (*Hordeum vulgare*; Varghese *et al.*, 1994; PDB entry 1ghs), banana (*Musa acuminata*; Receveur-Bréchot *et al.*, 2006; PDB entry 2cyg) and potato (*Solanum tuberosum*; Wojtkowiak *et al.*, 2012; PDB entries 3ur7 and 3ur8) and includes a central deep groove along the entire length of the upper surface of the molecule.

Although the overall fold of the endogenous Hev b 2 isoform II is highly conserved in the GH17 family, we found that it possesses unique structural features. Firstly, Hev b 2

contains an N-terminal pyroglutamate (Fuentes-Silva *et al.*, 2007), which is also found in numerous other PR proteins (Rep *et al.*, 2002) involved in resistance towards proteolysis and in protein–receptor interactions (Morty *et al.*, 2006). In plants, it has also been suggested that pyroglutamate is an important precursor and source of glutamate (Ohkama-Ohtsu *et al.*, 2008). A $2F_o - F_c$ electron-density map of this post-translational modification contoured at the 1.0$\sigma$ level is provided in Fig. 2(*a*). In Figs. 2(*b*), 2(*c*) and 2(*d*) we also present $2F_o - F_c$ electron-density maps of the glycosylation sites Asn27 and Asn314, which may possess the carbohydrate sequence shown in Fig. 2(*e*). This sequence has been found in several plant glycoproteins and was by far the most abundant sequence in this glycoallergen (92.5%; Supplementary Table S1). Secondly, the structure of Hev b 2 contains an Ω-like loop located on the protein surface (Ser96–Thr102) that is important for the association of the monomers in the asymmetric unit. This loop connects strand $\beta$4 (residues 85–94) to a small $3_{10}$-helix segment (residues 105–108; Fig. 1*c*). Notably, the side chain of Arg100 is highly exposed at the tip of the Ω-like loop and, interestingly, this position is occupied by Gly in most of the $\beta$-1,3-glucanase isoforms from *H. brasiliensis*. Thirdly, Hev b 2 contains additional structural elements in the C-terminal half of the barrel that include four short antiparallel $\beta$-strands and short helices and loops which constitute a small subdomain from strand $\beta$5 to helix $\alpha$6 (Fig. 1*c*) that is slightly larger than the subdomain reported for potato $\beta$-glucanase (Wojtkowiak *et al.*, 2012).

Notably, both asymmetric units ($P2_1$ and $P4_1$) exhibit a conserved dimer which buries a significant surface area at the interface that is stabilized by several interactions that involve Arg100 of one monomer and residues near the catalytic site of the opposite monomer (Fig. 3). These interactions vary among the different dimers and can include hydrogen bonds and salt bridges. For example, for the $P4_1$ crystal we observed the following interactions in the *B*–*C* dimer (Fig. 3*a*): Arg100*B* $N^{\omega}H1$ with Glu240*C* $O^{\varepsilon 1}$ (3.37 Å) and with Glu94C $O^{\varepsilon 2}$ (3.38 Å), Arg100*B* $N^{\omega'}H2$ with Tyr178*C* OH (3.53 Å), Arg100*B* $N^{\varepsilon}$ with Glu297*C* $O^{\varepsilon}$ (3.49 Å), Arg100*C* $N^{\omega}H1$ with Tyr178*B* OH (3.59 Å), Arg100*C* $N^{\omega'}H2$ with Glu297*B* $O^{\varepsilon 1}$ (2.78 Å) and with

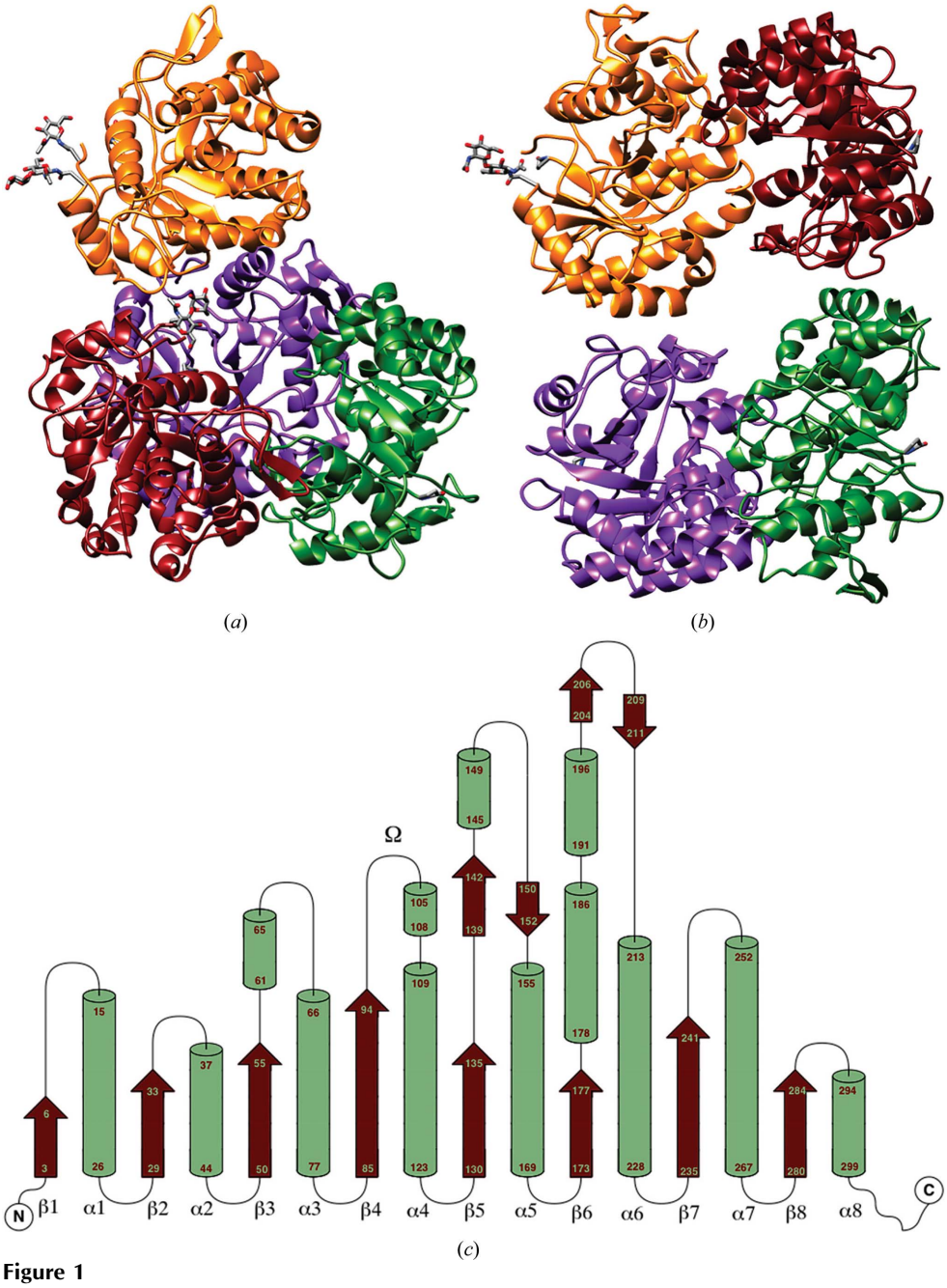


**Figure 1**
Quaternary structure adopted by endogenous Hev b 2 (endo-$\beta$-1,3-glucanase) in polymorphic crystals and the corresponding topology diagram. (*a*) Ribbon representation of the tetrahedral asymmetric unit arrangement in the monoclinic $P2_1$ crystal. Monomer *A* is shown in green, monomer *B* in red, monomer *C* in orange and monomer *D* in purple. (*b*) Ribbon representation of the $P4_1$ asymmetric unit that consists of a planar square assembly of two similar dimers (using an identical colour scheme). (*c*) Topology diagram of endo-$\beta$-1,3-glucanase from *H. brasiliensis*. $\beta$-Strands are coloured brown and helices are coloured green. An Ω-like loop is shown between $\beta$-strand 4 and a small segment of a $3_{10}$-helix. The dimers that were identified using the *PISA* web server are *A*–*D* in $P2_1$ and *A*–*D* and *B*–*C* in $P4_1$

Glu297*B* $O^{\varepsilon2}$ (3.52 Å), and Arg100*C* $N^{\varepsilon}$ with Glu297*B* $O^{\varepsilon1}$ (3.52 Å) and with Glu297*B* $O^{\varepsilon2}$ (2.70 Å) (Fig. 3*b*).

The same interface analysis for the *A*–*D* dimer ($P4_1$) is shown in Supplementary Fig. S3. In this dimer an energetically significant cation–$\pi$ interaction is found between Arg100*D* and Tyr178*A*, as determined using *CaPTURE* (Gallivan & Dougherty, 1999). Additionally, a short contact between Arg100D $N^{\omega'}$H2 and Glu297*A* $O^{\varepsilon1}$ (2.35 Å) was detected. Glu297 is located in the active site, close to the two catalytic residues (Glu94 and Glu240). This unusual distance could be explained by means of a 'short strong hydrogen bond', as reported in several unusual examples (Fuhrmann *et al.*, 2006; Frey, 2004). This could imply that the interaction between the two residues is emulating a transition state or an enzyme–intermediate complex. It has been reported that this type of enzymatic intermediate could exhibit 'short strong hydrogen bonds' with donor–acceptor distances below 2.50 Å (Cleland & Kreevoy, 1994). Nonetheless, theoretical calculations could provide a more exact description of this type of interaction.

It has been established that endo-$\beta$-1,3-glucanase from *H. brasiliensis* functions as a monomer, and its kinetic parameters (Churngchow *et al.*, 1995) and those of other $\beta$-glucanases, such as barley endo-$\beta$-1,3-glucanase, have been determined (Hrmova & Fincher, 1993; Hrmova *et al.*, 1995). We found that the Hev b 2 dimer was detected in solution only at concentrations higher than 0.15 mg $ml^{-1}$, at which the enzymatic activity toward laminarin is lost (results not shown). We also performed dynamic light-scattering (DLS) experiments that corroborated the presence of the dimer in solution using sodium citrate buffer pH 5.6 and a protein concentration of 0.5 mg $ml^{-1}$ (Supplementary Fig. S4). Based on these results, we suggest that the dimer plays an important role in the regulation of Hev b 2 activity in the lutoid bodies, in which the enzyme could exist as an inactive dimer; upon disruption of these organelles either mechanically or through insect or pathogen damage this defence enzyme adopts the monomeric and active conformation.

Finally, we detected three *cis*-peptides in all monomers ($P2_1$ and $P4_1$ crystals). Two were between residues Tyr144-Pro145 and Gln293-Pro294, which are located in solvent-exposed loops. A third, nonproline *cis*-peptide between Phe284 and Ala285 is found at the bottom of the groove that crosses the structure; interestingly, Phe284 lies parallel and adjacent to the catalytic residue Glu240 (at ∼3.90 Å). It has been reported that the *cis* and *trans* isomers provide stable local motifs that dramatically differ in structure, thereby providing a mechanism for selecting distinct binding partners even in the context of otherwise unstructured regions of proteins (Lu *et al.*, 2007). In this regard, evidence at the transcript level of the presence of a peptidyl–prolyl *cis*–*trans* isomerase in *H. brasiliensis* has been reported (UniProt B3FNQ1); however, no other *cis*–*trans* isomerase has yet been reported.

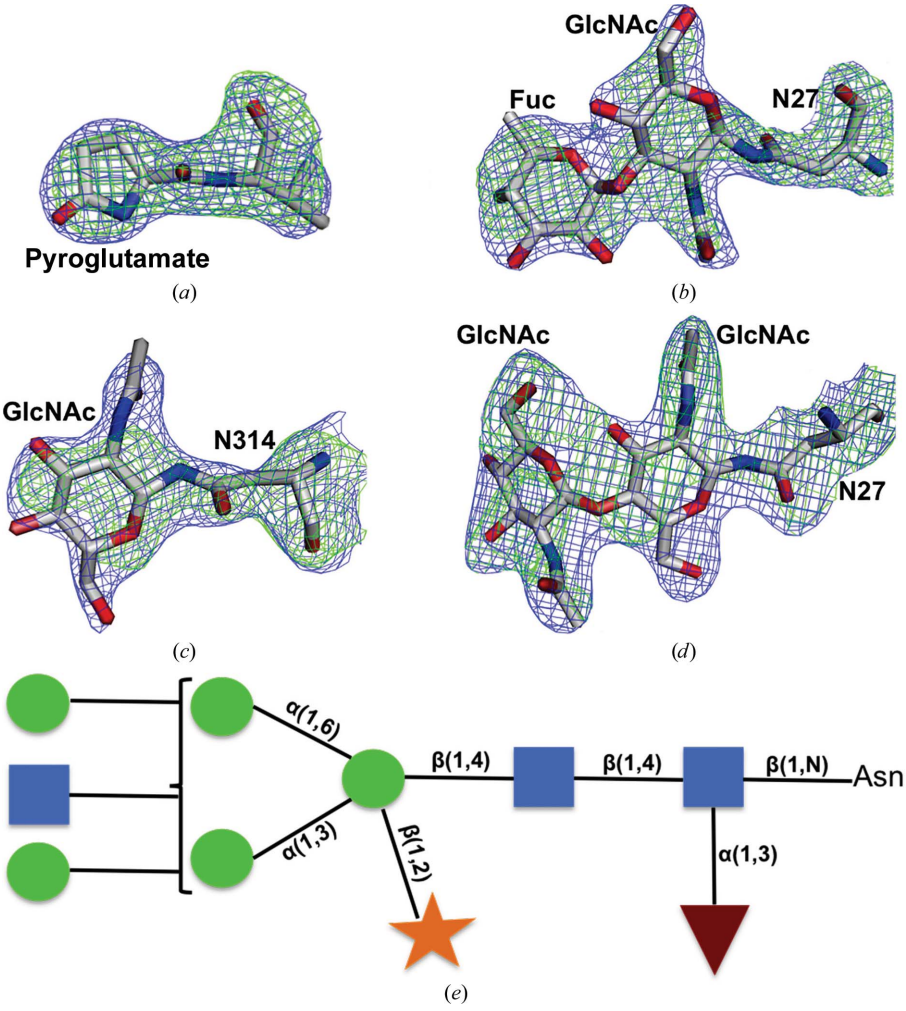


**Figure 2**
Post-translational modifications in Hev b 2. $2F_o - F_c$ and $F_o - F_c$ electron-density maps contoured at 1.0$\sigma$ and 3.0$\sigma$, respectively, showing the N-terminal pyroglutamate (monomer *C* in $P2_1$) (*a*) and the carbohydrate moieties at the two glycosylation sites: GlcNAc[Fuc($\alpha$1→3)] (monomer *B* in $P2_1$) (*b*), GlcNAc-Asn314 (monomer *C* in $P2_1$) (*c*) and GlcNAc[GlcNAc($\beta$1→4)] (monomer *C* in $P4_1$) (*d*). (*e*) The structure of the oligosaccharide that is present in Hev b 2 as determined in this work. The symbols and colours used are those recommended for drawing glycan structures (http://www.proglycan.com/upload/nomen_2007.pdf): GlcNAc, blue square; Fuc, red triangle; Man, green circle; Xyl, orange star.

### 3.2. Comparison with other $\beta$-1,3-glucanases

A superposition of the $C^{\alpha}$ atoms of the four monomers present in each asymmetric unit yields an average r.m.s.d. of 0.24 Å for the $P2_1$ crystal and 0.56 Å for the $P4_1$ crystal, as determined using *ALIGN* (Cohen, 1997), which indicates that the molecular structure of the monomers in each polymorph is

essentially identical. The superposition of chain *A* from the two polymorphs results in an r.m.s.d. of approximately 0.45 Å. The largest deviations occur at the surface loops that are involved in crystal contacts, such as Ser199–Tyr211, Pro275–Ala278 and Phe303–Gln309.

A structural comparison between Hev b 2 and other plant endo-$\beta$-1,3-glucanases that have been deposited in the PDB indicated several differences. The superposition of the $C^{\alpha}$ atoms of Hev b 2 and the allergenic banana $\beta$-1,3-glucanase (PDB entry 2cyg) results in the smallest r.m.s.d. (0.75 Å), whereas an r.m.s.d. of 0.86 Å was obtained upon superposition with the 1,3–1,4-$\beta$-glucanase from barley (PDB entries 1aq0 and 1ghr) and an r.m.s.d. of approximately 0.8 Å was obtained upon superposition with potato $\beta$-1,3-glucanase (PDB entries 3ur7 and 3ur8 for the free enzyme and 4gzj and 4gzi for the enzyme–carbohydrate complex; Fig. 4*a*). The potato $\beta$-1,3-glucanase contains an additional highly flexible subdomain that is part of the catalytic groove and that has been suggested to possibly be involved in substrate specificity (Wojtkowiak *et al.*, 2012). In Hev b 2, this flexible domain is larger and contains two pairs of short antiparallel $\beta$-strands and three short helical segments (Fig. 1*c*). An additional interesting feature of Hev b 2 is the presence of the aforementioned protruding Ω-like loop, which is involved in the dimerization of monomers (*A*–*D* in the $P2_1$ asymmetric unit and *A*–*D* and *B*–*C* in the $P4_1$ asymmetric unit). The potato $\beta$-glucanase conserves residue Arg123; however, the length of the loop is shorter and the conformation of the residue is different. Nevertheless, analysis of the structures of potato $\beta$-glucanase in the absence of substrates or products showed that residues of the His-tag octapeptide at the C-terminus of the enzyme occupy this position and interact with residues in the active site, mimicking substrate or product recognition (Wojtkowiak *et al.*, 2012).

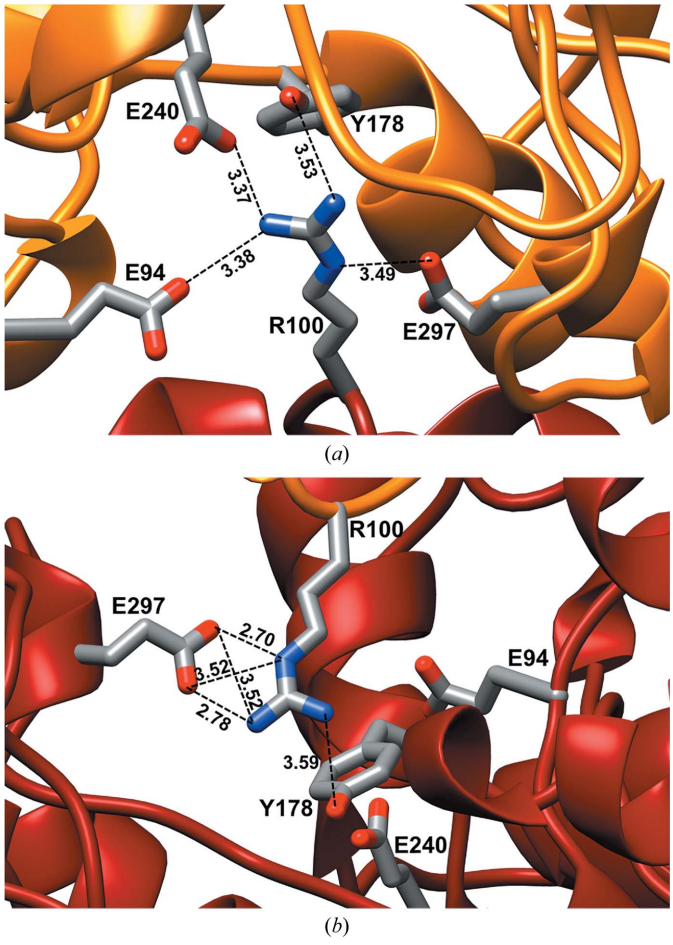


**Figure 3**
Ribbon representation of one of the Hev b 2 dimers in the $P4_1$ assembly (*B*–*C*). The two dimers found in the $P4_1$ crystal are similar. A detailed view of the interactions at the dimer interface is shown. Several salt bridges and hydrogen bonds (dashed lines) are observed and distances are indicated. Residues implicated in these interactions are labelled and shown as sticks; main chains are coloured according to the scheme described in Fig. 1. (*a*) Arg100 of monomer *B* and its interactions with monomer *C*. (*b*) Arg100 of monomer *C* and its interactions with monomer *B*.

Analysis of the coordinates of the two crystal forms using the *PISA* web server (http://www.ebi.ac.uk/msd-srv/prot_int/cgi-bin/piserver; Krissinel & Henrick, 2007) revealed that the only stable quaternary structure in the asymmetric unit is the dimer. For the monoclinic crystal the interface in the *A*–*D* dimer buries 1375 Å$^2$ with a $\Delta G$ of $-3.7$ kJ mol$^{-1}$. Intermolecular interactions within this interface are maintained by 16 hydrogen bonds and salt bridges that involve the Arg100 residues of the two polypeptide chains. For this crystal form there is one dimer in the asymmetric unit; however, symmetry-related contacts with molecules at $(-x, y + 1/2, -z)$ reproduced this interface. For the $P4_1$ crystal two protein–protein interface regions were analyzed: *A*–*D* and *B*–*C*. Both gave interface areas of 1338 Å$^2$ and a $\Delta G$ of $-3.1$ kcal mol$^{-1}$. Intermolecular interactions within the *A*–*D* interface are maintained by 26 hydrogen bonds and salt bridges, whereas 18 hydrogen bonds and salt bridges are present in the *B*–*C* interface.

### 3.3. The Hev b 2 active site

The hydrolysis of the glycosidic bond catalyzed by GH17 glycosidases is characterized by the retention of the stereochemistry of the anomeric C atom at the cleavage point (Jenkins *et al.*, 1995). In general, the overall topology of endo-$\beta$-1,3-glucanase active sites falls into the 'cleft or groove' open structure classification, which allows the random binding of several sugar units in polymeric substrates. Studies of the barley isozymes have indicated that there are eight subsites that accommodate glucosyl residues inside the catalytic groove (Hrmova *et al.*, 1995). The linear (1→3)-$\beta$-D-glucan substrate occupies subsites −3 to +5, with the scissile bond located between residues −1 and +1 (Davies *et al.*, 1998). It has been proposed that the hydrolysis reaction proceeds through a double-displacement mechanism involving a nucleophile and a proton-donor carboxylic group that are located on opposite sides of the hydrolyzed glycosidic bond at a distance of approximately 5.5 Å. Considering the recently proposed mechanism (Wojtkowiak *et al.*, 2013), the proton donor is situated within hydrogen-bonding distance of the

glycosidic O atom. After protonation of the glycosidic O atom by the proton donor, the nucleophile attacks the sugar ring from the opposite side relative to the leaving group to form a covalent glycosyl-enzyme intermediate, which is subsequently hydrolyzed by a water molecule in the next step of the reaction.

Several residues participate in the binding and hydrolysis of the substrates. Two conserved catalytic residues that act as the proton donor and the nucleophile correspond to Glu94 and Glu240, respectively, in the *H. brasiliensis* $\beta$-glucanase, and their location in the groove is shown in Fig. 4(*b*). Regarding other residues that are involved in substrate binding, a very recent report (Wojtkowiak *et al.*, 2013) presents two structures of potato endo-$\beta$-1,3-glucanase with an E259A mutation of the catalytic residue (Glu240 in Hev b 2) that unexpectedly hydrolyzed a hexasaccharide substrate into two different products: two trisaccharide molecules (PDB entry 4gzi) or a tetrasaccharide and a disaccharide (PDB entry 4gzj). From these structures the authors verified that conserved residues such as Asn117, Glu310, Lys313 and Glu319 interact with the glucose units at subsites −1 and −2 (corresponding to residues Asn93, Glu289, Lys292 and Glu297, respectively, in Hev b 2; Fig. 4*b*). In addition, several conserved aromatic residues are present in the groove that were found to directly interact with the oligosaccharides: Tyr58, Tyr201, Phe305 and Phe322 in potato $\beta$-glucanase (corresponding to Tyr34, Tyr178, Phe284 and Phe300 in Hev b 2, respectively; Fig. 4*b*). These results are corroborated by site-directed mutagenesis studies of barley $\beta$-1,3-glucanase (Chen *et al.*, 1995). Finally, it is noteworthy that in the structure of Hev b 2 we observed that Tyr144, which is present in one of the *cis*-peptide bonds (Tyr144-Pro145), adopts a conformation that occludes the carbohydrate-binding groove in some monomers (*A* in the $P2_1$ crystal and *D* and *B* in the $P4_1$ crystal; Fig. 4*b*, left panel), and therefore may be implicated in substrate specificity by regulating the timing of biological events such as protein–carbohydrate interactions or as part of the driving force for enzyme motion along the carbohydrate chain or of the polysaccharide along the groove. Besides, electron-density near Tyr144 (*A* in the $P4_1$ crystal) could be interpreted as an $Na^+$ ion. We included this ion on the basis of a proper cation–$\pi$ interaction (Dougherty, 2013),

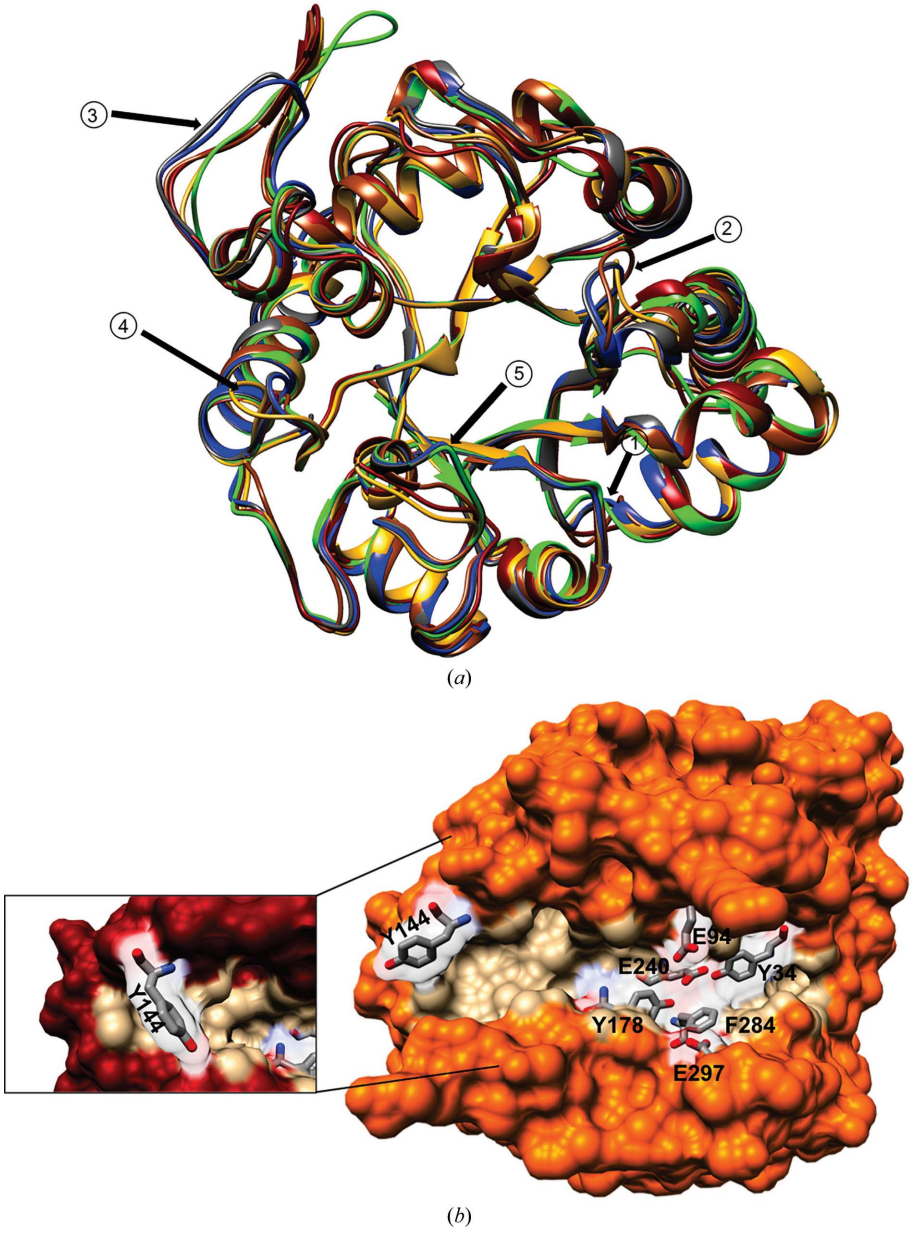


**Figure 4**
Overall fold of the biological monomer of Hev b 2. (*a*) Ribbon representation of several superimposed plant $\beta$-glucanases: Hev b 2 (monomer *A*, $P2_1$; brown), banana $\beta$-1,3-glucanase (PDB entry 2cyg; gold), barley $\beta$-1,3–1,4-glucanase (PDB entry 1aq0; red), barley $\beta$-1,3-glucanase (PDB entry 1ghs; green) and potato $\beta$-1,3-glucanase (PDB entries 3ur7 and 4gz1; without and with carbohydrates in the active site; grey and blue, respectively). Major differences are localized in the loops indicated by arrows. Using the numbering of Hev b 2, major differences lie in loop 1 (residues 80–85), loop 2 (94–103), which includes one catalytic residue and notably comprises the Ω-like loop that is only present in Hev b 2, loop 3 (residues 195–214), which exhibits the largest differences, loop 4 (residues 247–252) and loop 5 (residues 293–295). (*b*) Molecular surface of monomer *C* ($P4_1$ crystal). Catalytic residues (Glu94 and Glu240) and putative residues involved in substrate binding are shown in the right panel. The peptide bond of Tyr144 is in a *cis* configuration and adopts a conformation that occludes the carbohydrate-binding groove, as shown in the left panel (monomer *B*, $P4_1$).

appropriate behaviour during refinement and the presence of two sodium salts in the crystallization condition (0.2 *M* trisodium citrate and 0.1 *M* sodium cacodylate).

### 3.4. Carbohydrates and the role of glycosylation

N-linked glycan moieties of some glycoproteins from NRL and those from vegetables, fruits, pollens and insect venoms have been demonstrated to be involved in IgE-mediated allergy and cross-reactivity (Bonds *et al.*, 2008; Foetisch *et al.*, 2003; Tretter *et al.*, 1993). In general, oligosaccharides stabilize glycoproteins, protect them from proteases and prevent nonspecific protein–protein interactions; however, as previously mentioned, some oligosaccharides form specific recognition epitopes that affect receptor binding (Rudd *et al.*, 2004). A primary-structure analysis of Hev b 2 isoform II suggested one potential site for N-glycosylation at Asn27 and our previous biochemical studies indicated that approximately 6%(*w*/*w*) of the molecular mass could be attributed to carbohydrates (Fuentes-Silva *et al.*, 2007), which corresponds to approximately 14 saccharide units. In this study, we determined the N-linked glycan structure that is released from Hev b 2 through enzymatic digestion and identified nine different sugars (Supplementary Table S1). The most abundant glycan was the branched GlcNAc[Fuc($\alpha$1→3)]GlcNAcMan[Xyl($\beta$1→2]Man$_4$GlcNAc decasaccharide, which has been widely detected in other plant glycoproteins (Wilson *et al.*, 2001). Other identified glycans included high-mannose and $\alpha$1,6-fucosylated paucimannose forms (Supplementary Table S1).

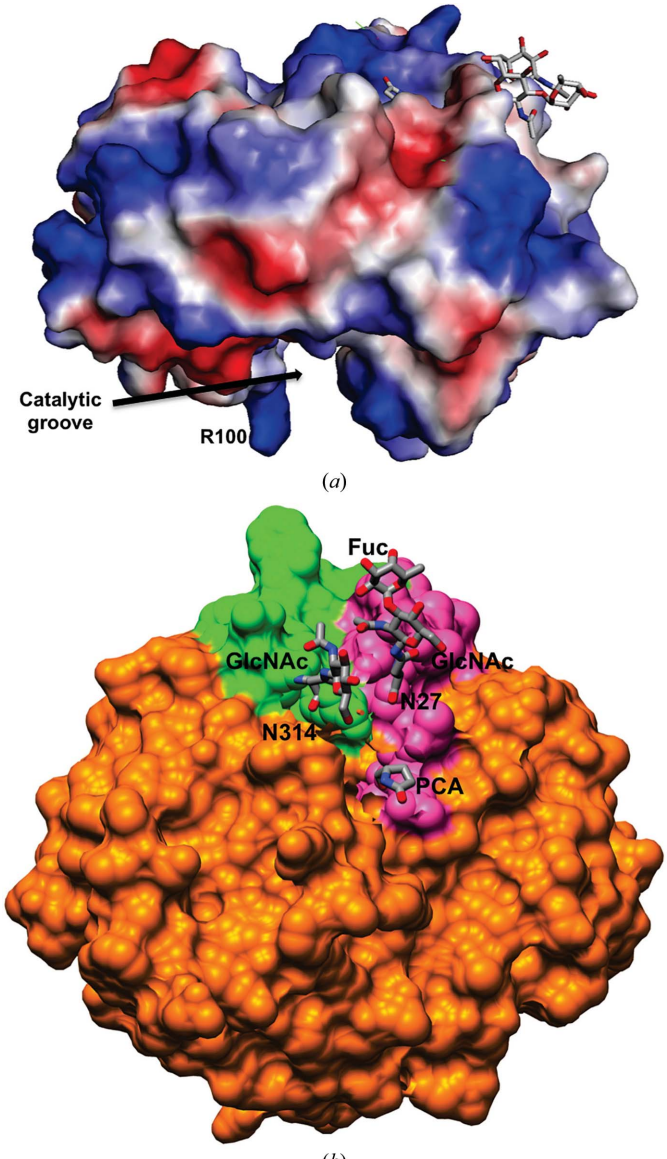


**Figure 5**
Location of putative IgE-binding epitopes. (*a*) Electrostatic potential surface of Hev b 2 (monomer *C*, $P2_1$ crystal). The three post-translational modifications are located in a patch on the surface of the protein that is surrounded by positively charged and some aromatic residues. On the opposite face of the protein the catalytic groove and residue Arg100, which is involved in protein dimerization, are also indicated. The volume of the groove based on the molecular surface is 609 Å$^3$ for Hev b 2, whereas the largest volume is observed for potato $\beta$-1,3-glucanase (PDB entry 4gzi) with bound carbohydrates (2916 Å$^3$). (*b*) Surface representation of the same monomer depicting the previously identified linear epitopes (putative epitopes 1 in green and 8 in pink; Barre *et al.*, 2009). Interestingly, these two epitopes contain the three post-translational modifications, which are shown as sticks, of the endogenous Hev b 2 allergen.

N-Glycosylation at Asn27 was evident from the electron-density maps of the $P2_1$ crystal, but the number of sugar units modelled in each of the four monomers differed. The largest carbohydrate was located at residue 27 in monomers *B* and *C* and consisted of a branched L-Fuc($\alpha$1→3)-GlcNAc disaccharide that could be modelled into the electron density (Fig. 2*b*); a third sugar residue, GlcNAc, that is attached to O4 of the first GlcNAc401*B* is observed at low contours but was not modelled. Poor electron density was observed for a single GlcNAc saccharide at residue 27 in monomers *A* and *D*, but the sugars were not included in the model. For the $P4_1$ crystal, we could only include a GlcNAc–GlcNAc disaccharide at Asn27 of monomer *C*. During model building and refinement we observed a clear excess of electron density at position Asn314 (Fig. 2*d*), which was not predicted to be an N-glycosylation site by the *NetNGlyc* server (http://www.cbs.dtu.dk/services/NetNGlyc); nevertheless, the residues involved included Asn-Phe-Ser, which is also considered to be a consensus sequence for N-glycosylation even though Thr is more common than Ser. At the Asn314 residue, we were able to model a single GlcNAc into the electron density for one monomer (*C*) in the $P2_1$ crystal and a clear excess of electron density was also visible in monomers *B* and *D* of the $P4_1$ crystal; however, no sugars were modelled owing to the low real-space correlation coefficient to electron density (RSCC) as determined in *PHENIX*.

As previously stated, the two N-glycosylation sites in Hev b 2 are localized at the sequon Asn27-Ile28-Thr29, whereas the second site was found at the sequon Asn314-Phe315-Ser316 at the C-terminus. The latter is not conserved in most of the *H. brasiliensis* $\beta$-1,3-glucanase isoforms, which predominantly contain the Asn314-Phe315-Gly316 sequon. Both glycosylation sites are spatially accessible on the surface of the protein and therefore may lead to a multivalent allergen, increasing the allergenic potency. The Hev b 2 crystal structure confirmed the presence of an N-linked branch

containing the L-Fuc($\alpha$1→3) residue, which was clearly interpreted in the $P2_1$ polymorph (monomers *B* and *C*).

The arrangement of residues found in the carbohydrate structure is similar to the highly immunogenic epitope of the Lewis$^X$ oligosaccharide. The Lewis$^X$ oligosaccharide D-Gal($\beta$1→4)-[L-Fuc($\alpha$1→3)]-$\beta$-DGalNAc-OH is a carbohydrate moiety that is commonly found in mammalian and nonmammalian complex glycans (Pérez *et al.*, 1996). Lewis$^X$-containing glycans are present in several human pathogens and are often associated with pathogen-induced TH2-biased adaptive immunity (Hsu *et al.*, 2007; Thomas, Hales *et al.*, 2003). The characteristic arrangement of residues found in our sugar structure differs slightly from the epitope of the Lewis$^X$ oligosaccharide, which has the Fuc residue $\alpha$1,3-linked to Asn-GalNAc instead of the $\alpha$1,3-fucosylation in Asn-GluNAc. Notably, it has been demonstrated that core $\alpha$1,3-fucosylation of the asparagine-linked GlcNAc of plant-derived (Altmann, 2007), snail-derived (van Tetering *et al.*, 1999) and insect-derived glycoproteins (van Ree *et al.*, 2000; Seismann *et al.*, 2010) is often associated with the allergenicity of such glycoproteins (van Ree *et al.*, 2000). Therefore, all of these findings suggest that this glycan epitope is a pan-allergen.

### 3.5. Potential IgE-binding epitopes in Hev b 2

Several attempts have been made to determine the distribution of epitopes within the amino-acid sequences of allergenic plant $\beta$-1,3-glucanases. For the banana $\beta$-glucanases, 15 linear or continuous IgE epitopes were predicted considering their hydrophilicity, flexibility and exposure to the solvent (Receveur-Bréchot *et al.*, 2006). More recently, nine IgE-binding epitopes along the amino-acid sequence of Hev b 2 were determined using synthetic 15-mer peptides (Barre *et al.*, 2009) and some of these epitopes coincided with those previously reported for the banana $\beta$-glucanases. Most of the amino-acid residues belonging to these IgE-binding epitopic regions are surface-exposed and typically correspond to charged regions on the molecular surface of the protein. For Hev b 2, it is noteworthy that although Arg100, which is located at the tip of the Ω-like loop, is highly exposed to the solvent, its presence in these epitopes was not predicted or observed by these authors (Barre *et al.*, 2009; Fig. 5*a*).

As a natural allergen, Hev b 2 preserves its endogenous carbohydrate moieties, which consist of two N-glycosylation sites, one of which contains L-Fuc($\alpha$1→3) and D-Xyl($\beta$1→2) residues similar to the branched Lewis$^X$-type motif. The three post-translational modifications are located on a patch exposed to the solvent and opposite the catalytic groove (Fig. 5*a*). Notably, both glycosylated Asn residues (27 and 314) belong to two linear epitopes that were previously proposed (Barre *et al.*, 2009; epitope 1, 16-VSEVIALYKKS**N**ITRMR IYDPNQA-39; epitope 8, 301-GLFFPNKWQKYNL**N**F-315) which are spatially near on the surface and form a conformational epitope (Fig. 5*b*). In this respect, notably, Hev b 2 dimerizes through interactions that involve the active-site groove, therefore leading to a divalent allergen that would enhance its allergenicity (Rouvinen *et al.*, 2010).

To determine the contributions of the carbohydrate moieties to the Hev b 2–IgE interactions, we utilized glycosylated and deglycosylated Hev b 2 isoform II in an ELISA test using 20 sera from symptomatic latex-allergic patients. The cutoff value (mean OD value ± 3s.d.) of the binding of five sera from non-allergic control subjects to Hev b 2 was 0.29 ± 0.02. As expected, all sera from latex-allergic patients

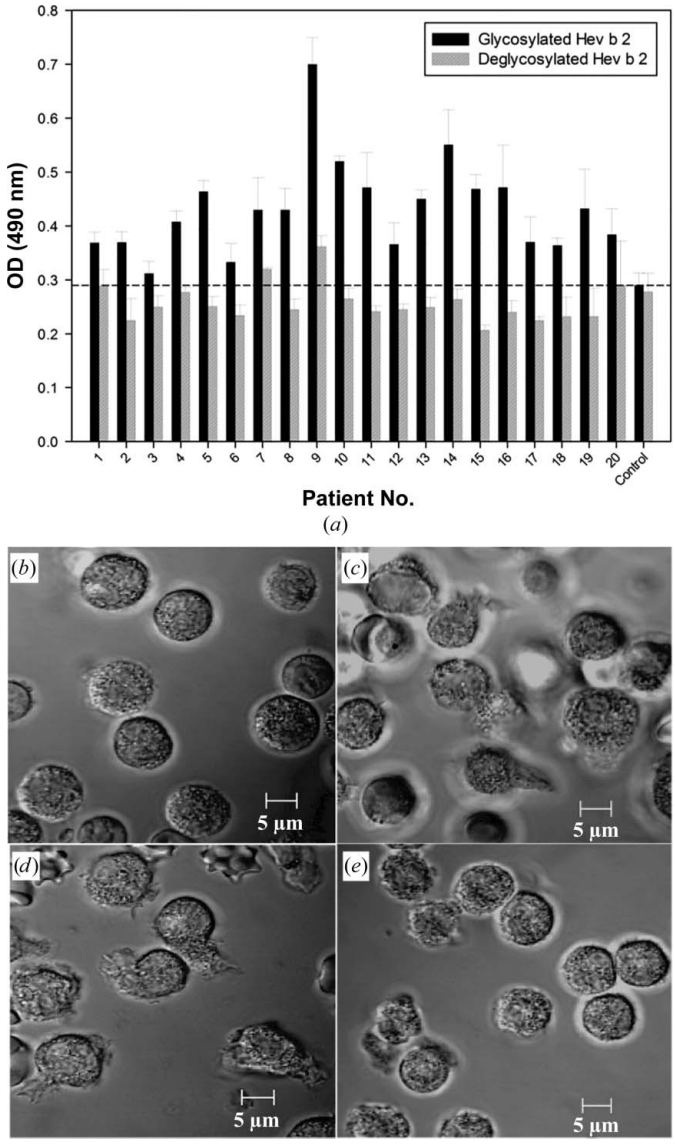


**Figure 6**
Enzymatic N-deglycosylation of Hev b 2 revealed that the glycan moieties produced an important decay of the allergen specific IgE binding. (*a*) ELISA experiments using sera from latex-allergic subjects. The ordinate axis shows the optical density (OD) at 490 nm. Black bars indicate IgE reactivity against the glycosylated Hev b 2, whereas white bars indicate IgE binding for the enzymatically deglycosylated form. Sera from five non-allergic voluntary donors were used as a control. Data represent the means of triplicate experiments. (*b*)–(*e*) Live-cell microscopic images of human sensitized basophils stimulated with two different latex allergens compared with non-stimulated basophils. Photomicrographs after 39 s of stimulation with each allergen are shown. (*b*) Non-stimulated basophils, (*c*) the allergen hevein (Hev b 6.02), (*d*) glycosylated Hev b 2 and (*e*) deglycosylated Hev b 2. Images were captured using a 40× objective on a confocal laser scanning microscope (Zeiss, LSM 510).

recognized the glycosylated protein, whereas the deglycosylated form failed to demonstrate significant binding to IgE in comparison with the control. Nevertheless, the reactivity of IgE towards deglycosylated Hev b 2 did not decay to the control level in two sera (Fig. 6*a*). These results agree with previous studies that suggested the possibility of a glycoepitope and/or a combined IgE-binding site that is composed of peptide and carbohydrate regions (Yagami *et al.*, 2002; Glesner *et al.*, 2011; An *et al.*, 2012).

To further confirm the importance of the *N*-glycan structures to basophil activation and degranulation, we used time-lapse video microscopy employing a Zeiss LSM 510 laser scanning microscope to monitor these processes after stimulation with the endogenous glycosylated and deglycosylated Hev b 2 allergen. Control non-stimulated but sensitized basophils did not demonstrate any morphological changes (Fig. 6*b*). We clearly observed that another major latex allergen, Hev b 6.02 (hevein; Reyes-López *et al.*, 2004), and the glycosylated form of Hev b 2 induced the activation and explosive degranulation of sensitized basophils after 39 s of treatment (Figs. 6*c* and 6*d*, respectively), confirming the ELISA results. Interestingly, deglycosylated Hev b 2 induced only a slight activation of the treated basophils (Fig. 6*e*). These results confirm that *N*-glycans contribute to the allergenicity of Hev b 2 and that carbohydrates are important immunogenic determinants, as has been found for other unrelated glycoallergens, such as those from tomato (Westphal *et al.*, 2003), cypress (Iacovacci *et al.*, 2002) and olive (Batanero *et al.*, 1999).

One interesting fact is the structural homology that exists between the glycan moieties on Hev b 2 and the Lewis$^X$ motif, which may function as a structural mimic or as a pathogen-associated molecular pattern (PAMP) that is recognized by different classes of pattern-recognition receptors (PRRs) such as Toll-like, C-type-lectin or mannose receptors. Interestingly, the Lewis$^X$ motif has been detected in the major secretory egg antigen from *Schistosoma mansoni* (IPSE/alpha-1) that activates human basophils (Wuhrer *et al.*, 2006). In fact, it has been demonstrated that the Lewis$^X$-type *S. mansoni* carbohydrate functions as an innate Th2 promoter *via* a particular L-Fuc($\alpha$1→3) residue that is required for this activity that also depends on TLR4 signalling (Thomas, Carter *et al.*, 2003). Other studies using extracts from *Aspergillus fumigatus* (Yamashita *et al.*, 2002) and the *S. mansoni* egg antigen (Meevissen *et al.*, 2010) have also indicated that carbohydrates can induce a T-helper type 2 (Th2) response. Accordingly, we suggest that the Hev b 2 oligosaccharides could interact with the TLR4 complex as Lewis$^X$-type ligands (Thomas, Carter *et al.*, 2003). In conclusion, the oligosaccharides present in glycosylated allergens may be a predominant target both in the innate immunity and the humoral immune response, and should be considered an important factor in their structural and immunochemical characterization.

The three-dimensional structure of Hev b 2 presented here is the first of an endogenous glycosylated allergen that is clinically relevant to latex allergy and cross-reactivity with other plant glycoallergens and insect venoms. Our results also confirmed that the glycan moieties present on Hev b 2 are an important allergenic IgE epitope and a possible elicitor of TLR4 or lectin-like receptor stimulation.

## 4. Conclusions

We present here the three-dimensional structure of the endogenous allergen Hev b 2, which is a $\beta$-1,3-glucanase belonging to the GH17 glycoside hydrolase family that exhibits the canonical $(\alpha/\beta)_8$ fold that is common in other plant $\beta$-1,3-glucanases such as those from barley, banana and potato. The structures of the two obtained crystal polymorphs show a dimer in the asymmetric unit, which revealed a possible regulatory mechanism through the occlusion of the active site by Arg100, which is present at the tip of an Ω-like loop.

Hev b 2 exhibits three post-translational modifications, including an N-terminal pyroglutamate and two glycosylation sites, one at Asn27 and another at Asn314. These modifications form a patch on the surface of the molecule that we propose to be the binding site for IgE antibodies. In addition, two IgE-binding epitopes that were previously identified (Barre *et al.*, 2009; the aforementioned epitopes 1 and 8) are coalescent on the molecular surface, creating extended IgE-binding areas on the surface of Hev b 2 which could play a key role in the allergenic potency. Our immunological studies suggest that the glycan moieties on Hev b 2, which are N-linked branched Lewis$^X$-type oligosaccharides, are important allergenic IgE epitopes.

Furthermore, confocal microscopy analysis and IgE-binding ELISA assays revealed the important role of the Hev b 2 carbohydrates in the induction of human allergenic reactivity against latex. These carbohydrate epitopes might be responsible for the IgE-binding cross-reactivity that is currently observed in latex–fruit syndrome. Overall, our results point out that the study of endogenous glycoallergens containing PAMP-type motifs, which cannot be obtained using recombinant proteins, is relevant to to the understanding of the wide adaptive and innate immune responses against allergens by the host. Thus, this type of analysis should be considered in the future design of allergy therapies and diagnostic tools.

This work was supported by DGAPA-UNAM (grant IN207613 to AR-R), CONACYT (grant 82947 to AR-R) and doctoral scholarship PB/0197 from DGEP-UNAM and CONACYT. We thank Georgina Espinosa-Pérez and Vanessa Hernández from the Instituto de Química and Instituto de Biotecnología, respectively, at UNAM for technical assistance and Vivian Stojanoff at the X6A beamline for assistance with X-ray data collection. The X6A beamline and the National Synchrotron Light Source, Brookhaven National Laboratory are funded by NIH–NIGMS under agreement GM-0080 and the US Department of Energy under contract No. DE-AC02-98CH10886, respectively. We are also very grateful to Dr Ezra Peisach from the RSCB PDB, Dr Lachele Foley from Glycam and Dr Nigel Moriarty from PHENIX for their help in the establishment of the correct sugar chirality and Dr Angel G.

Díaz-Sanchez for his help with the DLS experiments and for helpful discussions.

## References


Adams, P. D. *et al.* (2010). *Acta Cryst.* D**66**, 213–221.
Altmann, F. (2007). *Int. Arch. Allergy Immunol.* **142**, 99–115.
An, S., Chen, L., Wei, J.-F., Yang, X., Ma, D., Xu, X., Xu, X., He, S., Lu, J. & Lai, R. (2012). *PLoS One*, **7**, e31920.
Balasubramanian, V., Vashisht, D., Cletus, J. & Sakthivel, N. (2012). *Biotechnol. Lett.* **34**, 1983–1990.
Barre, A., Culerrier, R., Granier, C., Selman, L., Peumans, W. J., Van Damme, E. J., Bienvenu, F., Bienvenu, J. & Rougé, P. (2009). *Mol. Immunol.* **46**, 1595–1604.
Batanero, E., Crespo, J. F., Monsalve, R. I., Martín-Esteban, M., Villalba, M. & Rodríguez, R. (1999). *J. Allergy Clin. Immunol.* **103**, 147–153.
Bernstein, D. I., Biagini, R. E., Karnani, R., Hamilton, R., Murphy, K., Bernstein, C., Arif, S. A. M., Berendts, B. & Yeang, H. Y. (2003). *J. Allergy Clin. Immunol.* **111**, 610–616.
Blumchen, K., Bayer, P., Buck, D., Michael, T., Cremer, R., Fricke, C., Henne, T., Peters, H., Hofmann, U., Keil, T., Schlaud, M., Wahn, U. & Niggemann, B. (2010). *Allergy*, **65**, 1585–1593.
Bonds, R. S., Midoro-Horiuti, T. & Goldblum, R. (2008). *Curr. Opin. Allergy Clin. Immunol.* **8**, 82–86.
Bousquet, J., Flahault, A., Vandenplas, O., Ameille, J., Duron, J. J., Pecquet, C., Chevrie, K. & Annesi-Maesano, I. (2006). *J. Allergy Clin. Immunol.* **118**, 447–454.
Buss, Z. S. & Fröde, T. S. (2007). *J. Investig. Allergol. Clin. Immunol.* **17**, 27–33.
Chen, L., Garrett, T. P., Fincher, G. B. & Høj, P. B. (1995). *J. Biol. Chem.* **270**, 8093–8101.
Chen, V. B., Arendall, W. B., Headd, J. J., Keedy, D. A., Immormino, R. M., Kapral, G. J., Murray, L. W., Richardson, J. S. & Richardson, D. C. (2010). *Acta Cryst.* D**66**, 12–21.
Churngchow, N., Suntaro, A. & Witttsuwannnakul, R. (1995). *Phytochemistry*, **39**, 505–509.
Cleland, W. W. & Kreevoy, M. M. (1994). *Science*, **264**, 1887–1890.
Cohen, G. H. (1997). *J. Appl. Cryst.* **30**, 1160–1161.
Cremer, R., Lorbacher, M., Hering, F. & Engelskirchen, R. (2007). *Eur. J. Pediatr. Surg.* **17**, 194–198.
Davies, G. J., Mackenzie, L., Varrot, A., Dauter, M., Brzozowski, A. M., Schülein, M. & Withers, S. G. (1998). *Biochemistry*, **37**, 11707–11713.
Dougherty, D. A. (2013). *Acc. Chem. Res.* **46**, 885–893.
Emsley, P., Lohkamp, B., Scott, W. G. & Cowtan, K. (2010). *Acta Cryst.* D**66**, 486–501.
Evans, P. (2006). *Acta Cryst.* D**62**, 72–82.
Foetisch, K., Westphal, S., Lauer, I., Retzek, M., Altmann, F., Kolarich, D., Scheurer, S. & Vieths, S. (2003). *J. Allergy Clin. Immunol.* **111**, 889–896.
Fötisch, K. & Vieths, S. (2001). *Glycoconj. J.* **18**, 373–390.
Frey, P. A. (2004). *J. Phys. Org. Chem.* **17**, 511–520.
Fuentes-Silva, D., Mendoza-Hernández, G., Stojanoff, V., Palomares, L. A., Zenteno, E., Torres-Larios, A. & Rodríguez-Romero, A. (2007). *Acta Cryst.* F**63**, 787–791.
Fuhrmann, C. N., Daugherty, M. D. & Agard, D. A. (2006). *J. Am. Chem. Soc.* **128**, 9086–9102.
Galli, S. J., Nakae, S. & Tsai, M. (2005). *Nature Immunol.* **6**, 135–142.
Gallivan, J. P. & Dougherty, D. A. (1999). *Proc. Natl Acad. Sci. USA*, **96**, 9459–9464.
Garabrant, D. H., Roth, H. D., Parsad, R., Ying, G.-S. & Weiss, J. (2001). *Am. J. Epidemiol.* **153**, 515–522.
Gauchat, J.-F., Henchoz, S., Mazzei, G., Aubry, J.-P., Brunner, T., Blasey, H., Life, P., Talabot, D., Flores-Romo, L., Thompson, J., Kishi, K., Butterfield, J., Dahinden, C. & Bonnefoy, J.-Y. (1993). *Nature (London)*, **365**, 340–343.
Glesner, J., Wünschmann, S., Li, M., Gustchina, A., Wlodawer, A., Himly, M., Chapman, M. D. & Pomés, A. (2011). *PLoS One*, **6**, e22223.
Guile, G. R., Rudd, P. M., Wing, D. R. & Dwek, R. A. (1997). *A Laboratory Guide to Glycoconjugate Analysis*, edited by P. Jackson & J. Gallagher, pp. 199–234. Basel: Birkhauser.
Hrmova, M. & Fincher, G. B. (1993). *Biochem. J.* **289**, 453–461.
Hrmova, M., Garrett, T. P. & Fincher, G. B. (1995). *J. Biol. Chem.* **270**, 14556–14563.
Hsu, S.-C., Tsai, T.-H., Kawasaki, H., Chen, C. -H., Plunkett, B., Lee, R. T., Lee, Y. C. & Huang, S.-K. (2007). *J. Allergy Clin. Immunol.* **119**, 1522–1528.
Iacovacci, P., Afferni, C., Butteroni, C., Pironi, L., Puggioni, E. M., Orlandi, A., Barletta, B., Tinghino, R., Ariano, R., Panzani, R. C., Di Felice, G. & Pini, C. (2002). *Clin. Exp. Allergy*, **32**, 1620–1627.
Jenkins, J., Lo Leggio, L., Harris, G. & Pickersgill, R. (1995). *FEBS Lett.* **362**, 281–285.
Kabsch, W. (2010). *Acta Cryst.* D**66**, 125–132.
Krissinel, E. & Henrick, K. (2007). *J. Biol. Chem.* **372**, 774–797.
Kumar, R. P. (2012). *Indian J. Dermatol.* **57**, 66–70.
Leonard, E. J., Roberts, R. L. & Skeel, A. (1984). *J. Leukoc. Biol.* **35**, 169–177.
Leubner-Metzger, G. & Meins, F. (1999). *Pathogenesis-related Proteins in Plants*, edited by S. K. Datta & S. Muthukrishnan, pp. 49–76. Boca Raton: CRC Press.
Lu, K. P., Finn, G., Lee, T. H. & Nicholson, L. K. (2007). *Nature Chem. Biol.* **3**, 619–629.
Mahler, V., Gutgesell, C., Valenta, R. & Fuchs, T. (2006). *Clin. Exp. Allergy*, **36**, 1446–1456.
McCoy, A. J., Grosse-Kunstleve, R. W., Adams, P. D., Winn, M. D., Storoni, L. C. & Read, R. J. (2007). *J. Appl. Cryst.* **40**, 658–674.
Meevissen, M. H., Wuhrer, M., Doenhoff, M. J., Schramm, G., Haas, H., Deelder, A. M. & Hokke, C. H. (2010). *J. Proteome Res.* **9**, 2630–2642.
Miller, G. L. (1959). *Anal. Chem.* **31**, 426–428.
Min, B., Prout, M., Hu-Li, J., Zhu, J., Jankovic, D., Morgan, E. S., Urban, J. F. Jr, Dvorak, A. M., Finkelman, F. D., LeGros, G. & Paul, W. E. (2004). *J. Exp. Med.* **200**, 507–517.
Morty, R. E., Bulau, P., Pellé, R., Wilk, S. & Abe, K. (2006). *Biochem. J.* **394**, 635–645.
Ohkama-Ohtsu, N., Oikawa, A., Zhao, P., Xiang, C., Saito, K. & Oliver, D. J. (2008). *Plant Physiol.* **148**, 1603–1613.
Padilla, J. E. & Yeates, T. O. (2003). *Acta Cryst.* D**59**, 1124–1130.
Palomares, O., Villalba, M., Quiralte, J., Polo, F. & Rodríguez, R. (2005). *Clin. Exp. Allergy*, **35**, 345–351.
Peixinho, C. M., Tavares-Ratado, P., Gabriel, M. F., Romeira, A. M., Lozoya-Ibanez, C., Taborda-Barata, L. & Tomaz, C. T. (2012). *Br. J. Dermatol.* **166**, 518–524.
Pérez, S., Mouhous-Riou, N., Nifant'ev, N. E., Tsvetkov, Y. E., Bachet, B. & Imberty, A. (1996). *Glycobiology*, **6**, 537–542.
Pettersen, E. F., Goddard, T. D., Huang, C. C., Couch, G. S., Greenblatt, D. M., Meng, E. C. & Ferrin, T. E. (2004). *J. Comput. Chem.* **25**, 1605–1612.
Plum, M., Michel, Y., Wallach, K., Raiber, T., Blank, S., Bantleon, F. I., Diethers, A., Greunke, K., Braren, I., Hackl, T., Meyer, B. & Spillner, E. (2011). *J. Biol. Chem.* **286**, 43103–43111.
Receveur-Bréchot, V., Czjzek, M., Barre, A., Roussel, A., Peumans, W. J., Van Damme, E. J. & Rougé, P. (2006). *Proteins*, **63**, 235–242.
Ree, R. van, Cabanes-Macheteau, M., Akkerdaas, J., Milazzo, J. P., Loutelier-Bourhis, C., Rayon, C., Villalba, M., Koppelman, S., Aalberse, R., Rodriguez, R., Faye, L. & Lerouge, P. (2000). *J. Biol. Chem.* **275**, 11451–11458.
Rep, M., Dekker, H. L., Vossen, J. H., de Boer, A. D., Houterman, P. M., Speijer, D., Back, J. W., de Koster, C. G. & Cornelissen, B. J. (2002). *Plant Physiol.* **130**, 904–917.
Reyes-López, C. A., Hernández-Santoyo, A., Pedraza-Escalona, M., Mendoza, G., Hernández-Arana, A. & Rodríguez-Romero, A. (2004). *Biochem. Biophys. Res. Commun.* **314**, 123–130.

Rouvinen, J., Jänis, J., Laukkanen, M. L., Jylhä, S., Niemi, M., Päivinen, T., Mäkinen-Kiljunen, S., Haahtela, T., Söderlund, H. & Takkinen, K. (2010). *PLoS One*, **5**, e9037.
Royer, P. J., Emara, M., Yang, C., Al-Ghouleh, A., Tighe, P., Jones, N., Sewell, H. F., Shakib, F., Martinez-Pomares, L. & Ghaemmaghami, A. M. (2010). *J. Immunol.* **185**, 1522–1531.
Rudd, P. M., Wormald, M. R. & Dwek, R. A. (2004). *Trends Biotechnol.* **22**, 524–530.
Seismann, H., Blank, S., Braren, I., Greunke, K., Cifuentes, L., Grunwald, T., Bredehorst, R., Ollert, M. & Spillner, E. (2010). *Mol. Immunol.* **47**, 799–808.
Sokol, C. L., Barton, G. M., Farr, A. G. & Medzhitov, R. (2008). *Nature Immunol.* **9**, 310–318.
Tetering, A. van, Schiphorst, W. E., van den Eijnden, D. H. & van Die, I. (1999). *FEBS Lett.* **461**, 311–314.
Thomas, P. G., Carter, M. R., Atochina, O., Da'Dara, A. A., Piskorska, D., McGuire, E. & Harn, D. A. (2003). *J. Immunol.* **171**, 5837–5841.
Thomas, W. R., Hales, B. J. & Smith, W. (2003). *Clin. Exp. Allergy*, **33**, 416–418.
Tretter, V., Altmann, F., Kubelka, V., März, L. & Becker, W. M. (1993). *Int. Arch. Allergy Immunol.* **102**, 259–266.
Varghese, J. N., Garrett, T. P., Colman, P. M., Chen, L., Høj, P. B. & Fincher, G. B. (1994). *Proc. Natl Acad. Sci. USA*, **91**, 2785–2789.
Westphal, S., Kolarich, D., Foetisch, K., Lauer, I., Altmann, F., Conti, A., Crespo, J. F., Rodríguez, J., Enrique, E., Vieths, S. & Scheurer, S. (2003). *Eur. J. Biochem.* **270**, 1327–1337.
Wilson, I. B., Zeleny, R., Kolarich, D., Staudacher, E., Stroop, C. J., Kamerling, J. P. & Altmann, F. (2001). *Glycobiology*, **11**, 261–274.
Wojtkowiak, A., Witek, K., Hennig, J. & Jaskolski, M. (2012). *Acta Cryst.* D**68**, 713–723.
Wojtkowiak, A., Witek, K., Hennig, J. & Jaskolski, M. (2013). *Acta Cryst.* D**69**, 52–62.
Wuhrer, M., Balog, C. I., Catalina, M. I., Jones, F. M., Schramm, G., Haas, H., Doenhoff, M. J., Dunne, D. W., Deelder, A. M. & Hokke, C. H. (2006). *FEBS J.* **273**, 2276–2292.
Xiang, Z., Block, M., Löfman, C. & Nilsson, G. (2001). *J. Allergy Clin. Immunol.* **108**, 116–121.
Yagami, T., Osuna, H., Kouno, M., Haishima, Y., Nakamura, A. & Ikezawa, Z. (2002). *Int. Arch. Allergy Immunol.* **129**, 27–37.
Yamashita, Y., Okano, M., Yoshino, T., Hattori, H., Yamamoto, T., Watanabe, T., Takishita, T., Akagi, T. & Nishizaki, K. (2002). *Clin. Exp. Allergy*, **32**, 776–782.
Yeang, H. Y., Chow, K. S., Yusof, F., Arif, S. A., Chew, N. P. & Loke, Y. H. (2000). *J. Investig. Allergol. Clin. Immunol.* **10**, 215–222.